

# Isotopic composition of Hg and Pt in 5 slowly rotating HgMn stars <sup>\*</sup>

S. Hubrig<sup>1</sup>, F. Castelli<sup>2</sup>, and G. Mathys<sup>3</sup>

<sup>1</sup> University of Potsdam, Am Neuen Palais 10, D-14469 Potsdam, Germany

<sup>2</sup> CNR-Gruppo Nazionale Astronomia and Osservatorio Astronomico, Unita di Ricerca di Trieste, Via G.B. Tiepolo 11, Trieste, Italy

<sup>3</sup> European Southern Observatory, Casilla 19001, Santiago 19, Chile

Received xx / Accepted yy

**Abstract.** Theoretical models addressing the origin of peculiarities in the spectra of HgMn stars have not been sufficiently constrained so far by the available abundance data. Previous studies of Hg and Pt in samples of HgMn stars often relied on spectra of rather low resolution and low S/N ratio, so that only limited information could be derived from the centroid wavelength of unresolved isotopic blends. In this paper we present the results of a study of the isotopic compositions of Hg and Pt in 5 very slowly rotating HgMn stars. This work represents an improvement over previous studies due to the availability of very high spectral resolution ( $R = 118\,000$ ) and to the new information on wavelengths and atomic structure of Hg II and Pt II. Each of the observed stars has Hg overabundant by more than 5 dex compared with the solar abundance. The largest overabundance of Pt (4.59 dex) was found in the star HD 193452. No star shows terrestrial isotopic proportions. The most pronounced deviation from the terrestrial composition is found in the stars HD 141556 and HD 193452, which are the coolest ones in our sample.

**Key words:** Stars: abundances – Stars: atmospheres – Stars: chemically peculiar

## 1. Introduction

HgMn stars constitute a well-defined sub-group of chemically peculiar (CP) stars of late B spectral types. These stars exhibit marked abundance anomalies of several elements: e.g., overabundances of Mn, Ga, Y, Cu, Be, P, Bi, Sr, Zr, and deficiencies of He, Al, Zn, Ni, Co. In contrast to classical Bp and Ap stars, they generally have neither extreme overabundances of rare earths, nor significant overabundances of Si. Their spectral lines do not show conspicuous intensity variations. Neither have strong

large-scaled organized magnetic fields been definitely detected in any of them. More than 50% of the HgMn stars are members of either spectroscopic binary systems (SBs), many of which are double-lined systems (SB2s), or of systems of higher multiplicity, in which they are found in unusually high proportion (Hubrig & Mathys 1995).

Another important distinctive feature of these stars is their slow rotation ( $\langle v \sin i \rangle = 29 \text{ km s}^{-1}$ , Abt et al. 1972). The number of HgMn stars decreases sharply with increasing rotational velocity (Wolff & Wolff 1974). Evidence that stellar rotation does affect abundance anomalies in HgMn stars is provided by the rather sharp cutoff in such anomalies at a projected rotational velocity of 70–80  $\text{km s}^{-1}$  (Hubrig & Mathys 1996).

Many HgMn stars exhibit an extreme atmospheric overabundance of mercury: up to 5.7 dex (Smith 1997). The isotopic mix of Hg in HgMn stars differs from one star to the next, ranging from the terrestrial mix to nearly pure  $^{204}\text{Hg}$  (Cowley & Aikman 1975; White et al. 1976; Smith 1997). Heavier isotopes tend to dominate in cooler stars.

Besides mercury, other very heavy elements such as Pt (Dworetzky 1969; Dworetzky & Vaughan 1973) and Au (Wahlgren et al. 1994) are also overabundant in HgMn stars.

Dworetzky and Vaughan (1973) studied the line Pt II  $\lambda 4046$  in a sample of nine HgMn stars. In the nine stars studied, this line is shifted towards longer wavelengths, by 0.04 to 0.09 Å with respect to the centroid of the terrestrial platinum line. These shifts are interpreted as an isotopic effect. The corresponding anomalies are analogous to those found for Hg, with heavier isotopes predominant in cooler stars. However, without laboratory data for isotope shifts in Pt, no spectrum synthesis could be done at that time. Thanks to the availability of new laboratory measurements of isotope shifts in Pt II lines (Engleman 1989), it is now possible to interpret the observed Pt II isotope shifts in stellar spectra.

The theory advanced to explain the origin of anomalies in chemically peculiar stars, selective radiative diffusion, is

*Send offprint requests to:* G. Mathys

<sup>\*</sup> Based on observations obtained at the European Southern Observatory, La Silla, Chile (ESO programme No. 58.D-0654)

**Table 1.** Journal of observations

HD	Other id.	$V$	Sp. type	$\lambda$ range (Å)	HJD	S/N
35548	HR 1800	6.9	B9 HgMn	3965–4000	2450361.804	130
				4018–4053	2450362.836	140
141556	$\chi$ Lup	4.0	B9 YHg	4018–4053	2450360.487	230
				3965–4000	2450361.487	180
				3965–4000	2450363.486	280
158704	HR 6520	6.0	B9 MnHg	4018–4053	2450360.543	180
				3965–4000	2450361.539	150
193452	HR 7775	6.1	B9 HgPtSr	4018–4053	2450360.631	150
				3965–4000	2450361.624	180
216494	74 Aqr	5.8	B9 HgMn	4018–4053	2450360.703	110
				3965–4000	2450361.719	210
				3965–4000	2450363.551	210

dependent upon a fine balance of forces within the stellar line forming region (Michaud et al. 1974). However, neither it nor any other theory until now can satisfactorily account for the variations in the Hg and Pt isotope mix among the HgMn stars (Leckrone et al. 1993). On the other hand, theoretical models are not sufficiently constrained by the abundance data available until now for HgMn stars. Previous systematic studies of Hg and Pt in samples of HgMn stars relied on photographic spectra, or on CCD spectra of lower resolution than our data, so that only limited information could be derived from the centroid wavelength of unresolved isotopic blends.

The main purpose of the work reported here is to provide additional observational constraints to guide the theorists in the understanding of the isotopic anomalies in HgMn stars, improving upon previous studies through much better data quality.

## 2. Observations

The observations reported here have been performed at the European Southern Observatory with the 1.4 m CAT telescope and the CES Long Camera, equipped with CCD Loral #34. The spectra were recorded during 4 nights in October 1996 at a resolving power of 118 000. The wavelength ranges that were observed are 3965–4000 Å containing the line Hg II  $\lambda$  3984, and 4018–4053 Å containing three Pt II lines,  $\lambda\lambda$  4024, 4034, and 4046, and one Au II line,  $\lambda$  4052.6. The five selected stars all are sharp-lined stars with  $v \sin i$  below 4.0 km s<sup>-1</sup>. Programme stars are listed in Table 1, where we give the HD number and another identifier in Cols. 1 and 2, the  $V$  magnitude and the spectral type (both from the catalog of Renson et al. 1991) in Cols. 3 and 4, and for each observation, the wavelength range covered by the spectrum and the Heliocentric Julian Date of mid-exposure in Cols. 5 and 6. Spectra were reduced using MIDAS procedures, in a standard manner. The achieved signal-to-noise ratios in the continuum are

given in Col. 7 of Table 1. They were measured after reduction in portions of the spectrum apparently devoid of lines: accordingly the derived values must be regarded as lower limits of the S/N ratio actually obtained. It can be pointed out, however, that these values are in good agreement with those derived through statistical error evaluation from the consideration of the level of the recorded signal.

## 3. Spectral Analysis

Synthetic spectra and model atmospheres were computed with the SYNTHE and ATLAS9 codes (Kurucz 1997), respectively. Line lists are also from Kurucz (1995b). We only added the Pt II and Au II lines. Stellar parameters  $T_{\text{eff}}$  and  $\log g$  were derived by interpolating in the uvby $\beta$  grid of Strömgren indices computed for  $[M/H]=0.0$  from ATLAS9 models and fluxes (Castelli 1998). Observed indices were taken from the catalogue of Mermilliod et al. (1997) and were dereddened using the UVBYLIST code of Moon (1985). Table 2 lists the observed and dereddened Strömgren indices together with the derived stellar parameters. Column 12 specifies which indices were used to obtain  $T_{\text{eff}}$  and  $\log g$ . The definition of the indices  $a$  and  $r^*$  adopted for stars with parameters  $8500 \leq T_{\text{eff}} \leq 11000$  K and  $3.5 \leq \log g \leq 4.5$  can be found in the papers of Strömgren (1966) and Moon & Dworetzky (1985).

The errors associated to the parameters were derived by assuming an uncertainty of  $\pm 0.015$  mag for all the observed indices, except  $\beta$ , for which a probable error of  $\pm 0.005$  mag was adopted.

Adelman (1994) showed that most HgMn stars have little or no microturbulence. Therefore, for all the stars we assumed zero microturbulent velocity, while the rotational velocity was derived from the comparison of the observed and computed spectra, after having degraded the computed spectra for instrumental broadening. Last col-

**Table 2.** Strömgren indices and stellar parameters

HD	$(b - y)$	$(b - y)_0$	$m_1$	$m_0$	$c_1$	$c_0$	$\beta$	$E(b - y)$	$T_{\text{eff}}$ (K)	$\log g$	C.I.	$v \sin i$ ( $\text{km s}^{-1}$ )
35548	-0.009	-0.028	0.119	0.125	0.894	0.890	2.792	0.019	$11088 \pm 86$	$3.79 \pm 0.05$	$c_1 - \beta$	1.75
141556	-0.020	-0.022	0.129	0.130	0.948	0.948	2.841	0.002	$10664 \pm 400$	$3.98 \pm 0.04$	$a - r^*$	2.50
158704	-0.020	-0.055	0.117	0.129	0.577	0.570	2.757	0.035	$13163 \pm 124$	$4.22 \pm 0.05$	$c_1 - \beta$	2.50 <sup>1</sup>
193452	-0.007	-0.024	0.138	0.143	0.909	0.906	2.845	0.017	$10776 \pm 400$	$4.10 \pm 0.04$	$a - r^*$	2.00
216494	-0.038	-0.041	0.118	0.119	0.751	0.750	2.788	0.003	$11860 \pm 98$	$4.06 \pm 0.05$	$c_1 - \beta$	0.00

<sup>1</sup> See text.**Table 3.** Hg isotopic composition as determined from the analysis of Hg II  $\lambda$  3984 (isotopic fractions are given in %)

Isotope	$\lambda(\text{\AA})$	Terrestrial abundance	HD 35548 HR 1800	HD 141556 $\chi$ Lup	HD 158704 HR 6520	HD 193452 HR 7775	HD 216494 74 Aqr
196	3983.769	0.1504	0.00	0.00	0.00	0.00	0.00
198	3983.838	9.9968	0.16	0.00	1.00	0.00	7.02
199a	3983.838	7.14	0.32	0.00	3.00	0.00	6.19
199b	3983.849	9.71	0.44	0.00	15.5	0.00	9.29
200	3983.909	23.096	2.97	0.00	46.5	0.00	26.79
201a	3983.930	4.80	1.77	0.00	2.5	0.1	6.01
201b	3983.941	8.30	3.06	0.00	7.5	0.2	9.10
202	3983.990	29.863	50.58	1.00	22.2	49.6	26.79
204	3984.071	6.865	40.74	99.00	1.8	50.1	8.81
$\log(N_{\text{Hg}}/N_{\text{tot}})$ [Hg]		$-10.95_{\odot}$	$-5.70$ +5.25	$-5.50$ +5.45	$-5.85$ +5.10	$-5.35$ +5.60	$(-6.95)$

um of Table 2 lists the final rotational velocities which were used in computing the synthetic spectra.

For the double-lined spectroscopic binary HD 141556, an updated version of the BINARY code of Kurucz (1995a) was used to construct the final computed spectrum resulting from the contribution of both components. Following Wahlgren et al. (1994), we adopted  $R_A/R_B = 1.67$  for the ratio of the radii of the primary to the secondary stars, and  $T_{\text{eff}} = 9200$  K,  $\log g = 4.2$ , a microturbulent velocity  $\xi = 2.0$   $\text{km s}^{-1}$ , and  $v \sin i = 2$   $\text{km s}^{-1}$  for the secondary. Furthermore, we assumed solar chemical composition for this star, in spite of the fact that Wahlgren et al. (1994) derived abundances similar to those of an Am star, with deficiencies of Al, Si, Ca, and Sc and a large overabundance of Ba, but with nearly solar abundances for the iron peak elements. In fact, Wahlgren et al. (1994) reckoned the uncertainty of these determinations for the secondary “owing to either inherent weakness or blending with primary star lines”.

For the triple system HD 216494 (Hubrig & Mathys 1995), the fundamental parameters and chemical composition of the components are unknown. The analysis of this star was restricted to the study of the isotopic mixtures.

### 3.1. Mercury

The line Hg II  $\lambda$  3984 is observed in the spectra of all five studied stars.

We adopted  $\log gf = -1.73$  (Dworetzky 1980) for the whole transition responsible for the  $\lambda$  3984 line. For each isotopic component A, the oscillator strength is  $gf_A = gf N_A$ , where  $N_A$  is the fractional abundance of the isotope, while for each hyperfine component it is  $gf_{\text{hy p}} = gf_A I_A$ , where  $I_A$  is the relative strength of the hyperfine component. Terrestrial isotopic abundances (Anders & Grevesse 1989), and relative strengths of the hyperfine components (Smith 1997) are listed in Table 3.

For no star can the line Hg II  $\lambda$  3984 be fitted by the terrestrial isotopic composition, regardless of the Hg abundance. Therefore, we started by adopting the isotopic fractional model from White et al. (1976), according to which the stellar isotopic abundances are derived by means of the relation:

$$[N(A)/N(202)]_* = \alpha [N(A)/N(202)]_{\oplus}, \quad (1)$$

where  $\log \alpha = q(A - 202) \log e$ .  $q$  is a dimensionless mixture parameter and  $e$  is the base of the natural logarithms. It proved impossible to match satisfactorily the computed

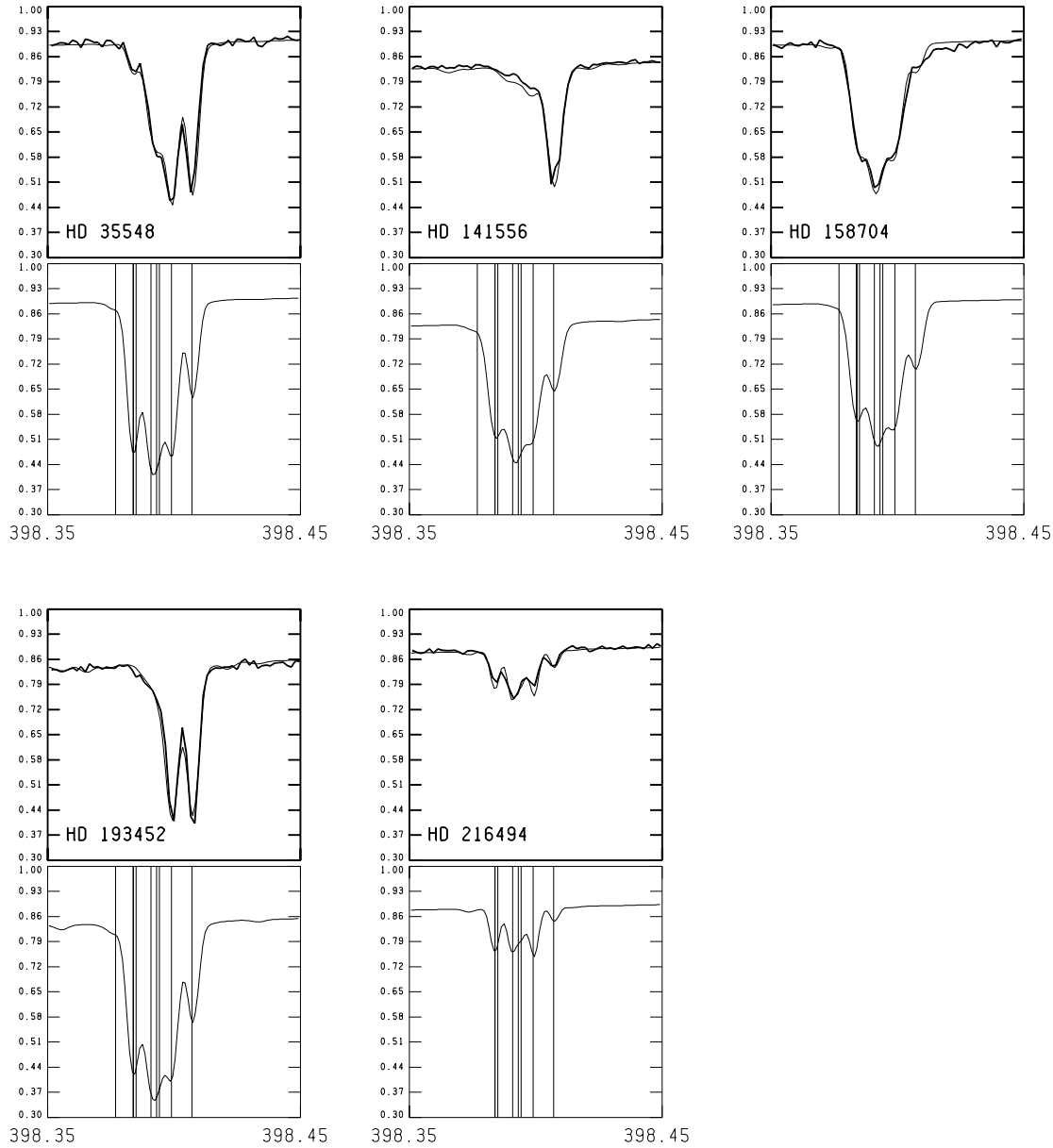


**Fig. 1.** Synthetic spectra (thin lines) computed with the Hg abundances and isotopic compositions summarized in Table 3 are compared with observations (thick lines). The ordinate is the normalized flux, and the abscissa is the wavelength in nm. For each star, below the comparisons, we show the expected profile for the same Hg overabundance, but for terrestrial isotopic composition. The vertical lines indicate the wavelengths of the different isotopic and hyperfine components

Hg II  $\lambda 3984$  profiles with the observed one using this approach. In other words, with high quality data, the fractional model of White et al. (1976) is found to be inappropriate. Accordingly, in a next step, we proceeded to modify the isotopic abundances by trial and error, until achieving the best fit of the observed profile.

For each star, Fig. 1 compares the observed spectra (thick lines) with synthetic spectra (thin lines) computed with the Hg abundances and isotopic compositions sum-

marized in Table 3. Below the comparison, the expected profiles for the same Hg stellar abundance, but for terrestrial isotopic composition are shown. The vertical lines indicate the wavelengths of the different isotopes and hyperfine components.

In Fig. 2, we compare the observed Hg II  $\lambda 3984$  line profile in the star HD 35548 (thick line) with the profile calculated by assuming the dimensionless mixture parameter  $q = 1.1$  (thin line) as given by Smith (1997). The

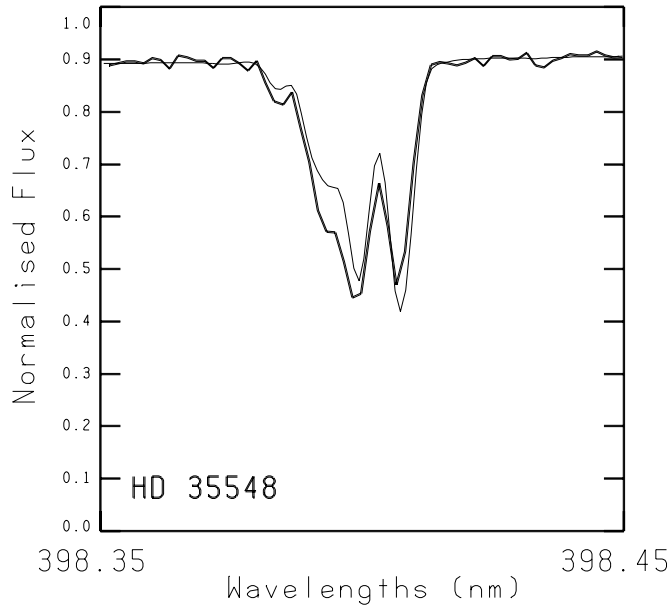


**Fig. 2.** Synthetic profile of the line Hg II  $\lambda$  3984 (thin lines) in the star HD 35548 computed with  $q=1.1$  is compared with the observed profile (thick line)

stellar parameters  $T_{\text{eff}}$  and  $\log g$ , the microturbulent and rotational velocities, and the overabundance of Hg were taken from the same paper. It is quite visible that the observed profile can not be reproduced satisfactorily by using the  $q$  parameter.

### 3.2. Platinum

Of the five stars observed, only HD 35548, HD 141556, and HD 193452 were found to show absorption lines of Pt II. We adopted  $\log gf = -2.61$ ,  $-2.09$ , and  $-1.19$  (Dworetsky et al. 1984), respectively, for the lines  $\lambda\lambda$  4023.8, 4034.2, and 4046.4. In Table 4, we present the transitions and energy levels given by Engleman (1989).

The isotopic shifts and hyperfine splittings for the isotopes 194, 195a, 195b, and 196 were measured by Engleman (1989). For the isotope 198 we used the relation

$$\lambda_{198} = \lambda_{194} - 2.086(\lambda_{194} - \lambda_{196}), \quad (2)$$

taken from Kalus et al. (1998). Terrestrial isotopic abundances were taken from Anders & Grevesse (1989), while the hyperfine intensities were obtained from Engleman's (1989) figures.

Because the line Pt II  $\lambda$  4046.4 is blended with Hg I  $\lambda$  4046.5, a proper analysis of the feature at 4046 Å must take into account both components of the blend. We adopted for Hg I  $\lambda$  4046.5 atomic data taken from Wahlgren et al. (1998), namely the isotopic and hyperfine structure listed in Table 5 and the total  $\log gf = -0.815$ . We used the Hg terrestrial and stellar isotopic abundances listed in Table 3.

**Table 4.** Transitions and energy levels for Pt II lines

$\lambda$ (Å)	Transition	$E_{\text{low}}$ ( $\text{cm}^{-1}$ )	$E_{\text{up}}$ ( $\text{cm}^{-1}$ )
4023.8	$6s \ ^2G_{7/2} - 6p \ ^4G_{9/2}^{\circ}$	29030.479	53875.493
4034.2	$6s \ ^2P_{3/2} - 6p \ ^4G_{5/2}^{\circ}$	32237.007	57018.130
4046.4	$6s \ ^4F_{5/2} - 6p \ ^4D_{5/2}^{\circ}$	36484.028	61190.026

**Table 5.** Hg I  $\lambda$  4046.5 isotopic wavelengths

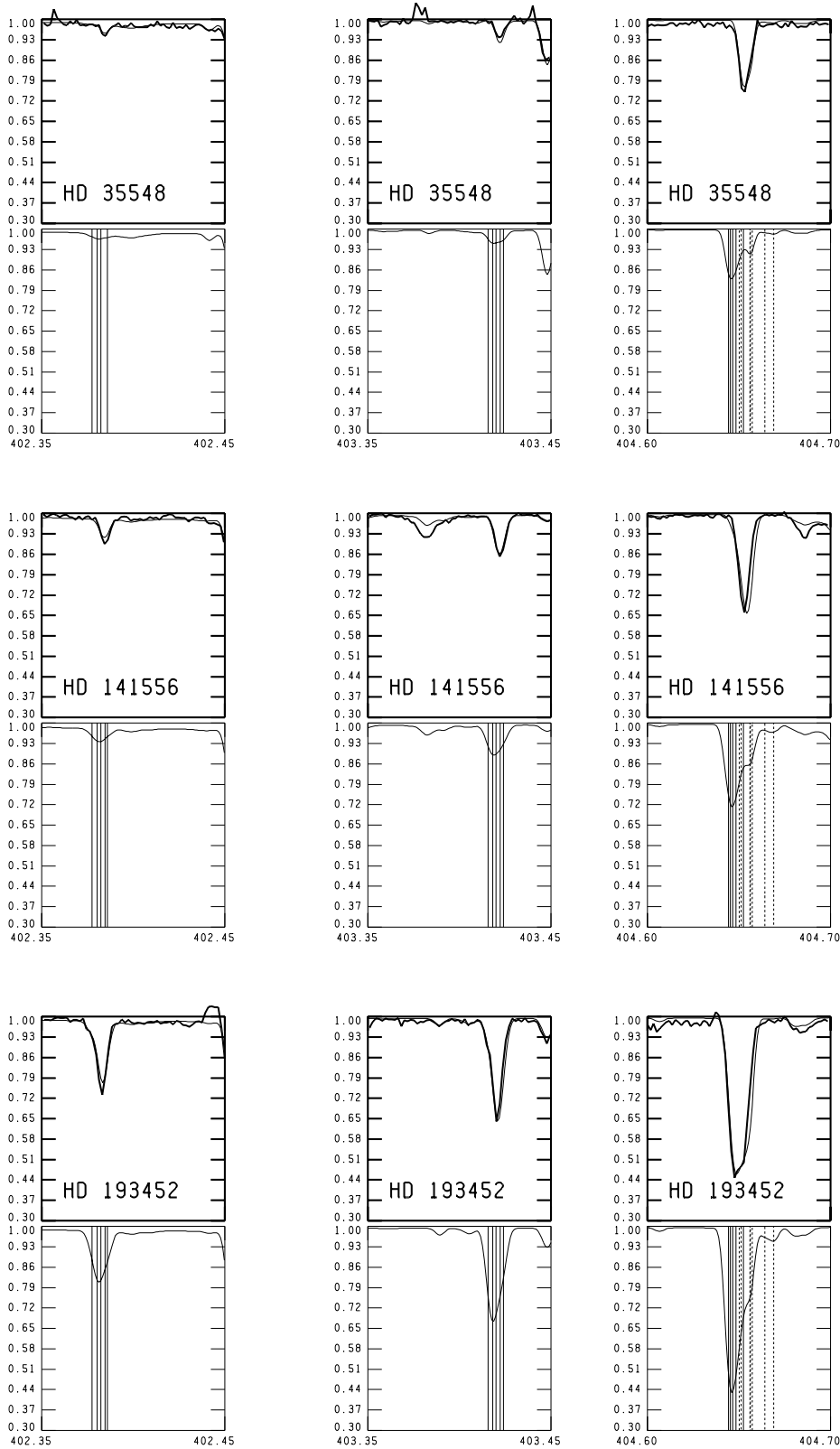
Isotope	$\lambda$ (Å)
198	4046.571
199a	4046.512
199b	4046.688
200	4046.569
201a	4046.501
201b	4046.609
201c	4046.675
202	4046.562
204	4046.559

Table 6 compares the terrestrial abundances of the individual isotopic components of the Pt II lines  $\lambda\lambda$  4023.8, 4034.2, and 4046.8 with the stellar abundances resulting from the line profile fitting. In each star, the same isotopic percentage for all three lines reproduces well the observed profiles.

Figure 3 compares, for each star, the observed spectra (thick lines) with synthetic spectra (thin lines) computed with the Pt abundances and isotopic compositions summarized in Table 6. Below, the expected profiles for the same Pt stellar abundance, but for terrestrial isotopic composition are shown. The vertical full lines indicate the positions of the Pt isotopes, while the dashed lines in the plots for the 4046–4047 Å region indicate the wavelengths of the isotopes and hyperfine components of the line Hg I  $\lambda$  4046.5; the contributions of the two hfs components 201b and 201c have been merged in a single component at 4046.642 Å.

### 3.3. Other elements

The wavelength ranges that were observed contain a number of spectral lines of other elements. In the process of computing the synthetic spectra, estimates of the abundances of these elements were obtained. Since the purpose of the present work is not the study of those abundances, no attempt was made to refine their determination or to assess the errors affecting them. Nevertheless, these abundance estimates, which in spite of their uncertainties, appear to be among the best constraints available for some of the considered species. Accordingly, they may be of interest to some readers, so that we are including them in Appendix A.



**Fig. 3.** Synthetic spectra (thin lines) computed with the Pt abundances and isotopic compositions summarized in Table 6 are compared with observations (thick lines). The ordinate is the normalized flux, and the abscissa is the wavelength in nm. For each star, below the comparisons, we show the expected profile for the same Pt overabundance, but for terrestrial isotopic composition. The vertical solid lines indicate the positions of the different Pt isotopic components, and the vertical dashed lines show the wavelengths of the isotopic and hyperfine components of the line Hg I  $\lambda$  4046.5

**Table 6.** Pt isotopic composition from the analysis of the lines Pt II  $\lambda\lambda$  4023.8, 4034.2, and 4046.4 (isotopic fractions are given in %)

Isotope	Component wavelengths ( $\text{\AA}$ )			Terrestrial abundance	HD 35548 HR 1800	HD 141556 $\chi$ Lup	HD 193452 HR 7775
	$\lambda$ 4023.8	$\lambda$ 4034.2	$\lambda$ 4046.8				
194	4023.803	4034.181	4046.443	32.9	0.00	0.00	0.00
195a	4023.774	4034.239	4046.466	19.1	0.00	0.00	10.00
195b	4023.858	4034.157	4046.453	14.74	0.00	0.00	7.50
196	4023.823	4034.200	4046.482	25.2	0.00	10.00	55.00
198	4023.845	4034.221	4046.524	7.19	100.00	90.00	27.50
$\log(N_{\text{Pt}}/N_{\text{tot}})$ [Pt]				$-10.24_{\odot}$	$-6.84$ $+3.40$	$-6.24$ $+4.00$	$-5.65$ $+4.59$

### 3.4. Uncertainties

There are several factors which affect the accuracy of the abundance determinations. Possible sources of errors include uncertainties in stellar  $T_{\text{eff}}$ ,  $\log g$ , and microturbulent velocity, and errors in the atomic data. We also discuss the rotational velocity of HD 158704.

Table 2 shows that the uncertainties of the temperatures derived from the photometric indices vary from star to star and may in the worst cases reach 400 K for the coolest stars. The gravity uncertainties from photometric determinations are less than 0.05 dex. But the gravities are furthermore affected by systematic errors as a result of the fact that they have been derived without taking into account the sub-solar helium abundances of the studied stars. The latter can be estimated by using the expression from Auer et al. (1966). We found  $\Delta \log g = -0.06$  dex for HD 141556 ( $[\text{He}/\text{H}] = [-0.20]$ ),  $-0.10$  dex for HD 193452 ( $[\text{He}/\text{H}] = [-0.90]$ ),  $-0.09$  dex for HD 35548 ( $[\text{He}/\text{H}] = [-0.50]$ ) and  $-0.11$  dex for HD 158704 ( $[\text{He}/\text{H}] = [-1.00]$ ).

We quantified the dependence of the Hg and Pt abundances on changes in the main stellar parameters by running multiple syntheses. We found that for all stars in our sample the derived abundances for Hg are not sensitive to errors of  $\pm 400$  K in effective temperature and  $\pm 0.1$  in surface gravity. Because the line Hg II  $\lambda$  3984 lies in the red wing of He $\epsilon$ , the error estimates were performed by assuming the He $\epsilon$  red wing as continuum for the Hg II line. In fact, the computed He profile changes if the stellar parameters are varied, but it can not be used to fix them, owing to the impossibility to draw a realistic continuum on the short wavelength range (3965–4000  $\text{\AA}$ ) covered by the observed spectrum.

Abundance errors for Pt due to errors in effective temperature and in surface gravity are of the order of 0.04 dex.

Uncertainty in the microturbulent velocity  $\xi$  introduces the largest errors in the abundances of Hg, but not of Pt. In fact, both Hg II  $\lambda$  3984 and Pt II  $\lambda$  4046 lie on the saturated portion of their curve of growth, so that a change of  $1 \text{ km s}^{-1}$  for  $\xi$  increases their equivalent widths. However, the lines Pt II  $\lambda\lambda$  4023 and 4034 are so weak

that they are unaffected by a change of  $\xi$ . The comparison of the abundances from these weak lines with that from Pt II  $\lambda$  4046 indicates that  $\xi = 0 \text{ km s}^{-1}$  is a good choice for HD 35548, HD 141556, and HD 193452. For the other star with no Pt lines, HD 158704, a microturbulent velocity  $\xi = 1 \text{ km s}^{-1}$  reduces by 0.15 dex the Hg abundance derived for  $\xi = 0 \text{ km s}^{-1}$ . Furthermore, the determination of the isotopic abundances is also affected by the choice of the microturbulent velocity. At higher microturbulence, the structure of Hg II  $\lambda$  3984 becomes much less resolved in the spectrum, so that we are no longer able to fit the abundances of the individual isotopic and hyperfine components.

The stars HD 35548, HD 141556, and HD 193452 have been subject to fine analyses in the past by different authors. Wahlgren et al. (1994) determined  $\xi = 0 \text{ km s}^{-1}$  for the primary star in the binary system HD 141556, Adelman (1994) derived  $\xi = 0 \text{ km s}^{-1}$  for HD 193452, and Smith gives  $\xi = 0.5 \text{ km s}^{-1}$  for HD 35548. The latter value,  $\xi = 0.5 \text{ km s}^{-1}$  in HD 35548, reduces by 0.1 dex the Hg abundance derived by us for  $\xi = 0.0 \text{ km s}^{-1}$ . The isotopic composition does not change significantly.

An important source of errors in the study of the Hg and Pt abundances is the oscillator strengths. The latter have estimated uncertainties of  $\pm 0.2$  dex for Hg II  $\lambda$  3984 (Dworetzky 1980), and of  $\pm 0.3$  dex for the Pt II lines (Dworetzky et al. 1984). Unfortunately, experimental values for Pt II lines do not exist at all. On the basis of the estimate  $\Delta \log N = -\log e \Delta f / f$  (Smith & Dworetzky 1993), errors on the derived abundances due to uncertainties in  $f$  may reach 0.25 dex for Hg and 0.43 dex for Pt.

The probable errors in the transition wavenumbers, isotopic shifts and hyperfine splitting are of the order of  $0.01 \text{ cm}^{-1}$  for Pt II (Engelmann 1989). Wavelengths of isotopic and hyperfine components for Hg II have been well known for a long time (Smith 1997 and references therein). They have been remeasured recently with the Lund Fourier Transform Spectrometer (Wahlgren 1998). The deviations with respect to the older values are in av-

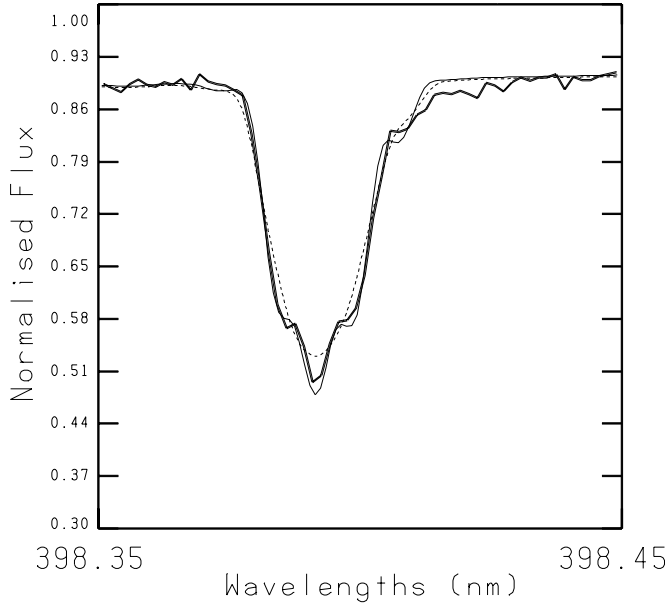


**Fig. 4.** Synthetic profiles for Hg II  $\lambda$  3984 for HD 158704 computed with  $v \sin i$  equal to  $2.5 \text{ km s}^{-1}$  (thin line) and  $4 \text{ km s}^{-1}$  (dotted line) compared with the observed profile (thick line)

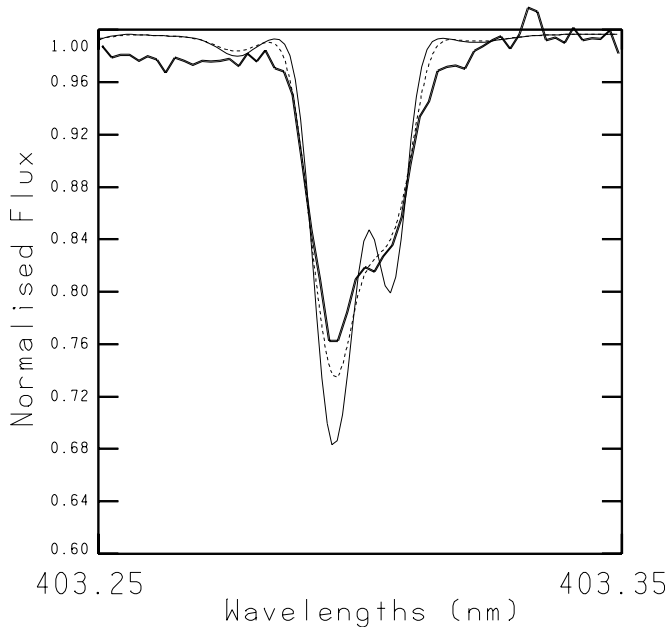


**Fig. 5.** Synthetic profiles for the blend Fe II, Ga I, Mn I at  $4032.9 \text{ \AA}$  in HD 158704 computed with  $v \sin i$  equal to  $2.5 \text{ km s}^{-1}$  (thin line) and  $4.0 \text{ km s}^{-1}$  (dotted line) compared with the observed profile (thick line)

erage of the order of  $2 \text{ m\AA}$ . For neither Pt II nor Hg II do these uncertainties contribute significantly to errors in the determination of the abundance and of the isotopic mixture.

Rotational velocities  $v \sin i$  were derived from the comparison of the observed profiles with computed profiles broadened with a rotational profile. The derived values

of  $v \sin i$  are usually well suited to reproduce all the profiles in the whole observed spectrum. However, in the case of HD 158704, the line Hg II  $\lambda$  3984 is much better reproduced by adopting  $v \sin i = 2.5 \text{ km s}^{-1}$ , rather than  $4 \text{ km s}^{-1}$ , as derived from all the other lines. We are currently unable to interpret the observed difference of apparent rotational velocity. We suggest that the discrepancy is due to some real physical effect, as yet unidentified. Since we do not know better, we felt compelled to adopt a pragmatic approach in the abundance analysis. Namely, we fitted the Hg line with  $v \sin i$  of  $2.5 \text{ km s}^{-1}$ , and the other lines with  $v \sin i$  of  $4 \text{ km s}^{-1}$ . We are aware that the resulting inconsistency increases the uncertainty of the abundances for HD 158704, but as long as we are not able to use a more satisfactory strategy, our approach should at least provide some roughly correct orders of magnitude for the abundances in this star. Figure 4 shows the differences between the Hg II  $\lambda$  3984 profiles computed with  $v \sin i$  equal to  $2.5 \text{ km s}^{-1}$  and  $4 \text{ km s}^{-1}$ . Figure 5 shows the same comparison for the feature at  $4032.9 \text{ \AA}$ , which is a blend of Fe II  $\lambda$  4032.935, Fe II  $\lambda$  4032.945, Ga I  $\lambda$  4032.976, and Mn I  $\lambda$  4033.062.

#### 4. Results and discussion

The four stars for which absolute abundances have been derived all have Hg overabundant by more than 5 dex compared with the solar abundance. The largest overabundance of Pt (4.59 dex) was found in the star HD 193452. No star shows terrestrial isotopic proportions. The most pronounced deviation from the terrestrial composition is found in the stars HD 141556 and HD 193452, which are the coolest ones in our sample. This result is in agreement with previous works on Hg and Pt (White et al. 1976; Dworetzky & Vaughan 1973; Smith 1997), that is, in the cooler stars both Hg and Pt are concentrated in their heaviest isotopes.

For two stars of our sample, HD 141556 and HD 193452, very extensive studies of abundances from space were carried out during the last years. In Table 7, we present our abundance determinations for Hg and Pt in these stars together with the abundances given by Smith (1997) and the abundances in the UV region given by Leckrone et al. (1998), Proffitt et al. (1998), and Kalus et al. (1998). The results in the UV region come exclusively from Goddard High Resolution Spectrograph (GHRS) observations.

For Hg II we derive an overabundance of 5.45 dex in HD 141556 which is higher than that determined in the UV region (5.00 dex). It is also higher than the abundance derived in the optical region from the line Hg I  $\lambda$  4358 (4.8 dex). We find similar results for the overabundance of Hg II in the star HD 193452. Proffitt et al. find an overabundance of Hg II of 5.3 dex whereas our analysis gives the value 5.65 dex.

**Table 7.** Studies of abundances of Hg and Pt in HD 141556 and HD 193452

	Hg I	Hg II	Hg III	Ref.	Pt I	Pt II	Pt III	Ref.
HD 141556								
UV transitions	+4.0	+5.1	+5.4	1	+3.9	+4.2	+4.5	2,3
optical transitions	+5.0	+5.3		4				
this paper		+5.45				+4.0		
HD 193452								
UV transitions		+5.3	+5.5	1		+4.7		3
this paper		+5.65				+4.59		

*References:* 1: Proffitt et al. 1998; 2: Leckrone et al. 1998; 3: Kalus et al. 1998; 4: Smith 1997

From the data of Proffitt et al. (1998), a trend of variation of the abundance with ionization stage is found in HD 141556. For HD 193452, these authors cannot draw any conclusion due to a lack of data. Such abundance discrepancies among ionization states probably result from a vertically stratified distribution of the given element within the observable outer layers of the star (Leckrone et al. 1998). It was also reported (Wahlgren & Dolk 1998) that in the star HD 193452, Hg isotopic shifts vary with the ionization stage.

By contrast, observations of Hg III  $\lambda\lambda$ 1738.47 and 1738.52 (Leckrone et al. 1993) in HD 141556 indicate that this ionization state is almost entirely in the form of the heaviest isotope: therefore no variation in isotopic shifts with the ionization stage is evident.

The difference between UV observations and our analysis in the optical region for Pt II for both stars is smaller than that for Hg II. We determine an overabundance of Pt II of 4.00 dex in HD 141556 and 4.59 dex in HD 193452. In the UV region, an overabundance of 4.25 dex was found for HD 141556, and of 4.70 dex (Kalus et al. 1998) for HD 193452. Interestingly, the identified platinum isotope mixture at optical wavelengths for the HgMn star HD 193452 appears to be different from that obtained from ultraviolet transitions (Wahlgren & Dolk 1998; Kalus et al. 1998).

## 5. Conclusion

Our high-resolution optical spectra have enabled us to study the abundances and isotopic composition of Hg and Pt in 4 slowly rotating HgMn stars. For the fifth star, the triple system HD 216494 (Hubrig & Mathys 1995), the fundamental parameters and chemical composition of the components are unknown. The analysis of this star was restricted to the study of the isotopic mixtures. The achieved results show that the Hg isotopic anomalies cannot be parameterized in a fractional model such as suggested by White et al. (1976). The isotopic mixture of Hg

and Pt had to be determined by trial and error. In agreement with previous works on Hg and Pt (White et al. 1976; Dworetzky & Vaughan 1973; Smith 1997), new determinations of isotopic anomalies in the optical spectra of sharp-lined HgMn stars show that in the cooler stars both Hg and Pt are concentrated in their heaviest isotopes. The largest overabundance of Pt (4.59 dex) was found in the star HD 193452. Isotopic abundances for Pt II have been derived from the consideration of three different lines. In each star, the same isotopic percentage for all three lines reproduces well the observed profiles.

In the case of HD 158704, the line Hg II  $\lambda$ 3984 is much better reproduced by adopting  $v \sin i = 2.5 \text{ km s}^{-1}$  rather than the value of  $4 \text{ km s}^{-1}$  derived from the rest of the spectrum. This seems to be due to some physical effect, which we are not able to identify at present, but which may prove to be important. The present observations do not allow us to decide if HD 158704 is a singular, isolated manifestation of this effect, or if it may be observable in other stars. Further observations of slowly rotating HgMn stars at high resolution and high S/N will have to be obtained to investigate whether the same physical effect is present in other stars.

Our work, when combined with UV observations with GHRS, provides additional data which should be used as constraints for diffusion models. Relative abundance variations and the variation of the isotopic composition among different ionization and excitation states of certain elements provide strong evidence for the effects of diffusion.

However, the number of stars for which abundances have been determined with accuracies better than the usual uncertainties of 0.2 to 0.3 dex by using both high S/N spectral data and very high resolution observations is still rather small. In order to adequately test the theory of radiative diffusion and element stratification, spectral lines need to be observed which arise from a range of excitation levels of the ions. Isotopic shifts should be observed for additional elements as well.

*Acknowledgements.* We are grateful to G.M. Wahlgren for useful discussions and comments on a preliminary version of this paper.

### Appendix A: Abundance estimates for other elements

As mentioned in Sect. 3.3, the synthetic spectra computed in the course of this study include fits of lines of various elements from which estimates of their abundances can be derived. These estimates are presented and briefly discussed below. It must be stressed that the results presented here should only be regarded as indicative of orders of magnitudes, but not as actual precise abundance values. Even so, they should prove useful for a number of applications.

The abundance estimates are summarized in Table A1. The crosses in the last column mean that corresponding elements are definitely present in the star HD 216494. In this table we do not indicate error limits for the abundances. Many synthesized lines are rather weak: consequently the derived abundances bear significant uncertainties.

In the following we comment the behaviour of some elements in studied stars.

In all five stars, He and Si are found to be strongly underabundant. This can be inferred from the intensity of the lines He I  $\lambda$  4046 and Si II  $\lambda\lambda$  4028.465 and 4035.278. However, the underabundances we found for Si II for HD 141556 ( $[-2.0]$ ) and for HD 193452 ( $[-2.0]$ ) do not agree at all with the Si II abundance for HD 141556 from Wahlgren et al. (1994) ( $[+0.14]$ ) and for HD 193452 from Adelman (1994) ( $[-0.05]$ ). The origin of the large discrepancy probably lies in errors in the  $\log gf$  values that we have adopted:  $-0.360$  for Si II  $\lambda$  4028.465, and  $-1.300$  for Si II  $\lambda$  4035.278. These values had to be taken from Kurucz & Peytremann's (1975) calculations, owing to the lack of any other better determination.

Mg was found underabundant only in HD 35548 on the basis of the only line Mg I  $\lambda$  3986.753. In the other stars, the line is neither observed nor predicted for solar abundance.

The phosphorus abundance was derived from the line P II  $\lambda$  4044.576. Phosphorus is overabundant in all the stars. The sulphur abundance was obtained from the line S II  $\lambda$  4028.750. This element is slightly overabundant in all the stars except for HD 158704, where it is slightly underabundant.

Overabundance for gallium in HD 158704, HD 193452, and HD 216494 was derived from the line Ga I  $\lambda$  4032.976. Although this line is heavily blended with Fe II and Mn I, it is well suited for Ga abundance estimation.

Yttrium was found to be strongly overabundant in all the stars but HD 216494, from consideration of the line Y II  $\lambda$  3982.594. In HD 216494 no lines of Y were observed. Few lines of Zr II indicate a moderate overabundance of this element in all the stars.

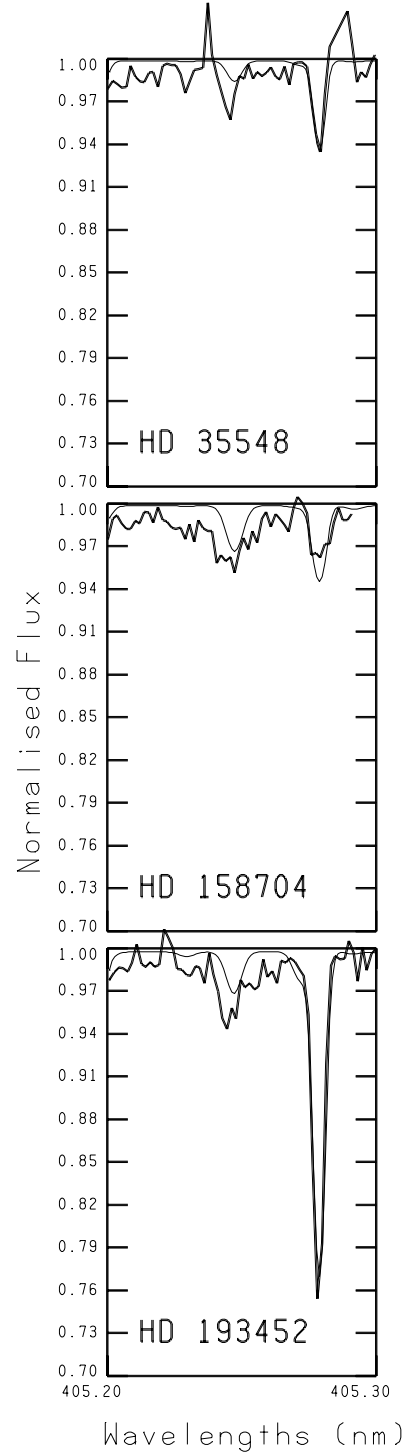


**Fig. A1.** Comparison of the computed (thin lines) and observed (thick lines) profiles of the line Au II  $\lambda$  4052.8

The observed spectral regions contains lines of the rare earth elements (REE) Ce ( $Z = 58$ ), Pr (59), Nd (60), Sm (62), Gd (64), Dy (66), and Ho (67). Several lines of Ce II and Pr II are listed in the line list of Kurucz (1995b) for

**Table A1.** Abundances  $\epsilon = \log(N_{\text{elem}}/N_{\text{tot}})$ 

Elem	HD 35548		HD 141556		HD 158704		HD 193452		HD 216494
	$\epsilon$	[M/H]	$\epsilon$	[M/H]	$\epsilon$	[M/H]	$\epsilon$	[M/H]	
He	-1.65	[-0.50]	-1.35	[-0.20]	-2.05	[-1.00]	-1.95	[-0.90]	
Mg	-5.26	[-0.80]							
Si	-6.59	[-2.10]	-6.49	[-2.00]	-6.50	[-2.10]	-6.49	[-2.00]	
P	-5.69	[+0.90]	-5.59	[+1.00]	-4.99	[+1.50]	-5.59	[+1.00]	×
S	-4.53	[+0.30]	-4.53	[+0.3]	-5.13	[-0.30]	-4.33	[+0.5]	
Ca	-5.88	[+0.20]	-5.48	[+0.2]	-4.48	[+1.20]	-5.00	[+0.68]	
Ti	-6.85	[+0.20]	-6.55	[+0.50]	-6.35	[+0.70]	-6.22	[+0.83]	
V	-8.54	[-0.50]	-8.04	[0.00]	-8.04	[0.00]	-7.84	[+0.20]	
Cr	-6.07	[+0.20]	-5.87	[+0.50]	-6.50	[-0.13]	-5.72	[+0.65]	
Mn	-5.55	[+1.10]	-6.65	[0.00]	-4.55	[+1.60]	-6.25	[+0.40]	
Fe	-4.63	[-0.10]	-4.27	[+0.26]	-4.20	[+0.33]	-4.15	[+0.38]	×
Ga			-9.16	[0.00]	-5.66	[+3.50]	-5.86	[+3.30]	
Y	-6.90	[+2.90]	-7.80	[+2.00]	-7.60	[+2.20]	-6.78	[+3.02]	
Zr	-8.54	[+1.00]	-9.04	[+0.50]	-8.04	[+1.55]	-9.24	[+0.30]	×
Ce	-8.49	[+2.00]	-8.59	[+1.9]	-7.49	[+3.00]	-8.69	[+1.80]	×
Pr	-8.33	[+3.0]	-8.33	[+3.0]	-7.33	[+4.00]	-8.33	[+3.00]	
Nd					-7.54	[+3.00]	-7.80	[+2.74]	×
Sm			-8.04	[+3.00]	-7.04	[+4.00]	-8.04	[+3.00]	
Gd	-9.92	[+1.00]	-9.02	[+1.90]	-8.22	[+2.70]	-8.82	[+2.10]	
Dy			-8.94	[+2.00]			-8.94	[+2.00]	
Ho	-8.98	[+2.80]	-9.58	[+2.20]	-7.98	[+3.80]	-8.98	[+3.00]	
Pt	-6.84	[+3.40]	-6.24	[+4.00]			-5.65	[+4.59]	
Au	-7.23	[+3.80]			-7.20	[+3.83]	-6.23	[+4.80]	
Hg	-5.70	[+5.25]	-5.50	[+5.45]	-5.85	[+5.20]	-5.35	[+5.60]	
U							-9.51	[+3.00]	

the studied region. But in none of the stars they can be observed with an intensity larger than the noise. We estimated Ce and Pr abundances by assuming the very weak features to be real lines. Accordingly, the numbers derived are upper limits. Lines of Nd II can be observed without any doubt in the spectra of HD 193452 and HD 216494. Nd is probably also overabundant in HD 158704. In this star, some predicted lines agree well with the observed ones, but others are weaker than the observed lines. Inaccuracies of the  $\log gf$  values cannot be excluded. No lines of Sm II can be observed in HD 35548, while in the other stars, this ion could be identified as very weak features, such as those at 4037.105 Å and 4042.709 Å. Lines of Gd II are present in the spectra of HD 141556 and HD 193452, and probably in the spectrum of HD 158704. If Gd is present in HD 35548, it is observable only at the level of the noise. We used mostly the lines Gd II  $\lambda\lambda$  4049.423 and 4049.855 to check the presence of Gd and to derive its abundance. In both HD 141556 and HD 193452, Dy II is seen as a weak blend with a line of Fe I at 4032.470 Å. The derived abundance yields other predicted lines of Dy II generally in good agreement with the observed spectra. The line  $\lambda$  4045.474 is the only Ho II line present in the line list for the 3970–4050 Å region. On the basis of this only line, we identified Ho in all the stars, except HD 216494. The line

is very weak and blended. It is at the level of the noise in HD 141556 and HD 158704.

A very weak feature at the level of the noise in HD 193452 at the position of U II  $\lambda$  4050.041 might possibly indicate an overabundance of this element in this star. Better observations are needed to settle this point.

The weak line Au II  $\lambda$  4052.8 is in the observed wavelength range for three stars, HD 35548, HD 158704, and HD 193452. It has been used to derive the abundance of gold, another heavy element enhanced in the HgMn stars. For one HgMn star, HD 193452, a gold overabundance of 4.8 dex was derived, which is the largest one found among HgMn stars until now. Figure A1 shows the comparison of the observed and computed Au II profiles for the three stars. Until recently, gold abundance had been determined from UV lines for four HgMn stars (Wahlgren et al. 1993) and for the hotter peculiar star Feige 86 (Bonifacio et al. 1995). New atomic data for Au II lines in the visual (Rosberg & Wyart 1997) have allowed us to estimate the abundance of gold from our visible region spectra.

## References

- Abt H.A., Chaffee F.H., Suffolk G., 1972, ApJ 175, 779  
Adelman S.J., 1994, MNRAS 266, 97  
Anders E., Grevesse N., 1989, Geochim. Cosmochim. Acta 53, 197

- Auer L.H., Mihalas D., Aller L.H., Ross, 1966, *ApJ* 145, 153  
Bonifacio P., Castelli F., Hack M., 1995, *A&AS* 110, 441  
Castelli F., 1998, in preparation  
Cowley C.R., Aikman G.C.L., 1975, *PASP* 87, 513  
Dworetsky M.M., 1969, *ApJ* 156, L101  
Dworetsky M.M., 1980, *A&A* 84, 350  
Dworetsky M.M., Vaughan A.H., 1973, *ApJ* 181, 811  
Dworetsky M.M., Storey P.J., Jacobs J.M., 1984, *Phys. Scr.* T8, 39  
Engleman R.J., 1989, *ApJ* 340, 1140  
Hubrig S., Mathys G., 1995, *Comments Astrophys.* 18, 167  
Hubrig S., Mathys G., 1996, *A&A* 120, 457  
Kalus G., Johansson S., Wahlgren G.M., Leckrone D.S., Thorne A.P., Brandt J.C., 1998, *ApJ* 494, 792  
Kurucz R.L., 1995a, CD-ROM No. 18. *Smithsonian Astrophys. Obs.*, Cambridge, MA.  
Kurucz R.L., 1995b, CD-ROM No. 23. *Smithsonian Astrophys. Obs.*, Cambridge, MA.  
Kurucz R.L., 1997, private communication  
Kurucz R.L., Peytremann E., 1975, *SAO Special Rep.* 362  
Leckrone D.S, Wahlgren G.M., Johansson S., Adelman S.J., 1993, Exploring abundance and isotope anomalies in CP stars with the HST/GHRS: High resolution UV spectroscopy of  $\chi$  Lupi. In: Dworetsky M.M., Castelli F., Faragiana R. (eds.), *Proc. IAU Coll. 138, Peculiar versus Normal Phenomena in A-Type and Related Stars.* *Astron. Soc. Pacific Conf. Series Vol. 44*, p. 42  
Leckrone D.S, Johansson S., Wahlgren G.M., Proffitt C.R., Brage T., 1998, GHRS spectroscopy of chemically peculiar stars: The  $\chi$  Lupi pathfinder project. In: Brandt J., Petersen C.C., Ake T. (eds.), *GHRS Science Symposium* *Astron. Soc. Pacific Conf. Series*, in press  
Mermilliod J.C., Mermilliod M., Hauck B., 1997, *A&AS* 124, 349  
Michaud G., Reeves H., Charland Y., 1974, *A&A* 37, 313  
Moon T.T., 1985, *Commun. Univ. London Obs.* 78  
Moon T.T., Dworetsky M.M., 1985, *MNRAS* 217, 305  
Proffitt C.R., Brage T., Leckrone D.S., Wahlgren G.M., Brandt J.C., Reader J., Johansson S., 1998, *ApJ*, in press  
Renson P., Gerbaldi M., Catalano F.A., 1991, *A&AS* 89, 429  
Rosberg M., Wyart J.-F., 1997, *Phys. Scr.* 55, 690  
Smith K.C., 1997, *A&A* 319, 928  
Smith K.C., Dworetsky M.M., 1993, *A&A* 274, 335  
Strömgren B., 1966, *ARA&A* 4, 433  
Wahlgren G.M., 1998, private communication  
Wahlgren G.M., Dolk L., 1998, *Contrib. Astron. Obs. Skalnaté Pleso*, p. 314  
Wahlgren G.M., Leckrone D.S., Johansson S., Rosberg M., 1993, Using HST/GHRS echelle spectra as template for IUE data analysis. In: Dworetsky M.M., Castelli F., Faragiana R. (eds.), *Proc. IAU Coll. 138, Peculiar versus Normal Phenomena in A-Type and Related Stars.* *Astron. Soc. Pacific Conf. Series Vol. 44*, p. 121  
Wahlgren G.M., Adelman S.J., Robinson R.D., 1994, *ApJ* 434, 349  
Wahlgren G.M., Dolk L., Kalus G., Johansson S., Litzen U., 1998, *ApJ*, submitted  
White R.E., Vaughan A.H., Preston G.W., Swings J.P., 1976, *ApJ* 204, 131  
Wolff S.C., Wolff R.J., 1974, *ApJ* 194, 65